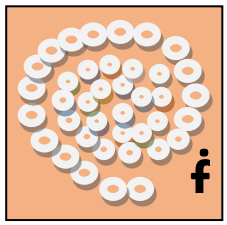

International Journal of Mathematical Analysis and Modelling

(Formerly Journal of the Nigerian Society for Mathematical Biology)

Volume 8 Issue 2, 2025

ISSN (Print): 2682 - 5694
ISSN (Online): 2682 – 5708
www.tnsmb.org

Numerical solution of fractional order COVID-19 model via the generalized fractional Adams-Bashforth-Moulton approach

T.U. Onoja*, J. Amos†, W. Atokolo‡§, E. Abah¶, D. Omale‖, G.O. Acheneje **and B. Bolaji††

Abstract

The objective of the paper is to conduct an inquiry of a few of the epidemiological characteristics of COVID-19 infection by invoking a fractional-order mathematical framework in measuring the impact of vaccination and treatment to the dynamics of the spread of COVID-19. It qualifies the conditions of existence and uniqueness of the solution of the model in the fractional repetition and stabilities the endemic equilibrium by the use of the method of the Lyapunov function. The sequence of numerical simulations that used the fractional Adams-Bashforth Moulton approach elaborates on the role played by the chosen model parameters, and the fractional-orders values improving the control and dynamics of COVID-19. Additional mathematical simulations that utilize surface and contour plots indicate that the prevalence of COVID-19 would be higher in case of higher contact rates and lower efficiency of treatment. The study further establishes that an optimal strategy on vaccination and treatment would end up countering the high rate of COVID-19 among the population.

Keywords and phrases: COVID-19; fractional; Stability; numerical simulation.

1 Introduction

The COVID-19 pandemic is an infectious disease that emerged late in the year 2019 in Wuhan, China [1] due to a coronavirus known as SARS-CoV-2 which is the reason leading to the illness that has been transmitted to other parts of the globe. Laplace-Adomian Decomposition Method (LADM) proposed in [1] in its fractional-order sterile insect technology (SIT) model was used to control proliferation of Zika virus whose solutions were in an infinite series converging to the exact solution. COVID-19 can be spread by inhalation of infectious agents or contact with the eye, nose, and mouth. The risk is the greatest when being in the immediate vicinity, yet very small particles of the air transporting the virus can remain in the air longer and move further, particularly, in enclosed spaces. Another way the germs can be passed, is through touching an infected surface or object and subsequently touching the eyes,

*E-mail: tuonoja@gmail.com; Department of Mathematical Sciences, Prince Abubakar Audu University, Anyiba, Nigeria
†Department of Mathematical Sciences, Prince Abubakar Audu University, Anyiba, Nigeria; E-mail: amosjeremiah1997@gmail.com
‡Corresponding Author; E-mail: williamsatokolo@gmail.com
§Department of Mathematical Sciences, Prince Abubakar Audu University, Anyiba, Nigeria
¶Department of Mathematical Sciences, Prince Abubakar Audu University, Anyiba, Nigeria; E-mail: abahemmanuel1995@gmail.com
‖Department of Mathematical Sciences, Prince Abubakar Audu University, Anyiba, Nigeria; E-mail: davidubahi@gmail.com
**Department of Mathematical Sciences, Prince Abubakar Audu University, Anyiba, Nigeria; E-mail: achenejegodwin@gmail.com
††Department of Mathematical Sciences, Prince Abubakar Audu University, Anyiba, Nigeria: bolarinwa.s.bolaji@gmail.com

nose or mouth. People are infectious until 20 days and are capable of spreading the virus despite the fact that they are not manifesting the symptoms of the disease. [2] used the mathematical modeling that was a fractional order to respond to the various epidemiological profiles of the Lassa fever viral infection to define how Lassa fever infection treatment and vaccination would affect the Lassa fever epidemic dynamics transmission using a fractional order derivative with power law that allows to work better. disease dynamics.

The series solutions in terms of LADM was determined in regard to a fractional-order compartmental model of Caputo derivative to an example of soil-transmitted helminth infection with several series solutions formed. They have identified that the infinite series converged to the exact solution and the fractional-order model was more flexible as compared to classical one. [1] have formulated a fractional-order SIT model to reduce the Zika virus spread where they use LADM to find an analytical solution. They also demonstrated that the fractional model is less rigid since they had alternative responses discretion to alter the fractional order. What makes their contribution to the literature is the ability to demonstrate how LADM can be applied to solving SIT models, which is a new thing in the area of research. Adopted from a fractional-order model of the dynamic of COVID-19 and Monkey pox co-infection transmissions [3], LADM was applied to approximate solutions, and the results found were fitted to real-life data. They considered that at an increased treatment capacity, burden of disease would be minimized. [4] have conducted the analysis of the effect of parameter values; the influence of (θ), (ϕ), h, and (γ) on decreasing of basic reproduction number (R0) of COVID-19 means that there is the possible effect of manipulation of these parameters that can one day eliminate the disease in the population. Their modeling effort revealed that good execution of control predictive measures such as social distancing, use of hand hygiene and cough etiquette would aid in the elimination of the disease over time. Additionally, the quarantine, isolation of suspect and confirmed cases is also an effective option to reduce pandemic.

Using Adams-Bashforth-Moulton method, [5] developed a fractional mathematical model of the dynamics of hepatitis C transmission. They found that decreased contactrates and improved treatment were a major preventative of the spread of the disease with the fractional-order model offering better flexibility than any classical methods. The dynamics of transmission of HIV/AIDS were also modeled in [6] by using a set of fractional-order models using the Adams-Bashforth-Moulton form of integration method. The results of their study showed that reducing the rate of contacts and enhancing the treatment approaches were successful to take the diseases under control and showed the elevated flexibility of the fractional models over the conventional counterparts. The work in [7] also provided an Adams-Bashforth-Moulton approach and gave a fractional-order model of Diphtheria transmission. Their findings proved the fact that a decrease in a contact rate and an increase in the effectiveness of treatment suppressed the process of spreading the disease, displaying once more the benefits of fractional-order models to describe intricate systems as compared to classical.

There is a considerable advantage of the fractional-order model owing to its flexibility and non-locality. Fractional derivatives unlike its classical counterparts are able to better model true data and reflect non-locality an issue with classical derivatives. The memory effect is one of the distinguishing characteristics of fractional-order models and is impossible to be achieved with the classical ones since fractional operators are deemed to be unusual. One of the more recent ways in which a great number of researchers have approached these problems is through fractional differential equations. Among the noteworthy is the research work of [8] whose interest is to come up with a solution of fuzzy volterra integral equations with degenerate kernels through a hybrid technique that makes use of both Laplace transform and Adomian Decomposition Method. The methodology has gained significance in terms of what it adds to the theory on fuzzy analytical dynamic equations whose outcomes are incisive. Existence and stability of a three point boundary value problem was also done in[8], where the different types of Ulam stability have been pursued by looking at classical methods of non-linear fraction analysis.

The objectives of this paper are to:

- Determine conditions of the existence and uniqueness of solution of the fractional model.

- Examine the stability of the endemic equilibrium point by the means of the Lyapunov function method.
- item Get numerical solutions by fractional Adams-Bashforth-Moulton method.
- Perform numerical grid based simulations of the model.

Reading the papers on the mathematical model of COVID-19 and transmission dynamic, we have found no study on transmission dynamic and control of COVID-19 based on fractional calculus with the application for numerical simulation of the Adams-Bashforth-Moulton method.

The remainder of this paper is organizationally presented as follows: in Section 2 a description of the formation of the model is explained, Section 3 presents the analysis of the model developed, Section 4 offers the numerical analysis of the fractional-order model and lastly, Section 5 makes concluding statements.

1.1 Preliminary

Here we provide the basic outcomes and definitions of fractional calculus. In this paper we will use the right and left fractional Caputo derivative [9, 10]. Also in this manuscript, the use of fractional calculus in the modeling of real problems in physics, engineering, bio-mathematics as well as other fields of science is highlighted.

Definition 1

let $f \in \Lambda^{\infty}(R)$, then the left and right Caputo fractional derivative of the function f is given by

$$\begin{aligned} {}^{c}D_{t}^{\gamma} f(t) &= \left({}_{t}^{0}D_{t}^{-(m-\gamma)} \left(\frac{d}{dt} \right)^{m} f(t) \right) \\ {}^{c}D_{t}^{\gamma} f(t) &= \frac{1}{\Gamma(m-\gamma)} \int_{0}^{t} \left((t-\lambda)^{m-\gamma-1} f^{m}(\lambda) \right) d\lambda \end{aligned} \tag{1}$$

The same way

$${}_{T}^{c}D_{t}^{\gamma} f(t) = \left({}_{t}D_{T}^{-(m-\gamma)} \left(\tfrac{-d}{dt} \right)^{m} f(t) \right)$$

$${}_{T}^{c}D_{T}^{\gamma} f(t) = \tfrac{(-1)^{m}}{\Gamma(m-\gamma)} \int_{t}^{T} \left((\lambda - t)^{m-\gamma-1} f^{m}(\lambda) \right) d\lambda$$

Definition 2

The generalized Mittag-Leffler function $E_{\alpha,\beta}(x)$ for $x \in R$ is given by

$$E_{\alpha,\beta}(x) = \sum_{m=0}^{\infty} \frac{x^{m}}{\Gamma(\alpha m + \beta)}, \ \alpha, \beta > 0 \tag{2}$$

which can also be represented as

$$E_{\alpha,\beta}(x) = x E_{\alpha,\alpha+\beta(x)} + \frac{1}{\Gamma(\beta)} \tag{3}$$

$$E_{\alpha,\beta}(x) = L\left[t^{\beta-1} E_{\alpha,\beta(\pm\psi t^{\alpha})} \right] \ = \frac{S^{\alpha-\beta}}{S^{\alpha} \pm \psi} \tag{4}$$

Proposition 1.1

Let $f \in \Lambda^{\infty}(R) \cap C(R)$ and $\alpha \in R,\ m-1 < \alpha < m,$

therefore, the conditions given below holds:

- ${}_{t_0}^{c}D_t^{\gamma} I^{\gamma} f(t) = f(t)$
- $I_{t_0}^{\gamma} D_t^{\gamma} f(t) = f(t) - \sum_{k=0}^{m-k} \frac{t^k}{k!} f^k(t_o)$.

1.2 Model formulation

In developing the COVID-19 integer-order model, the population is divided into seven groups: Susceptible individuals (S);(those free from the infection),Exposed individuals (E_C) (those not yet infectious); Quarantine population (Q_C) (those who are quarantined), ; Infected population (I_C) (those infected with COVID-19) ; Isolated population.

(I_{TC}) (the people that are under treatment but not yet healed) , Vaccinated population (V_C) population of those who were vaccinated against COVID-19 and Recovered population (R_C) population of those people that have recovered due to COVID-19. The recruitment of COVID-19 Susceptible Individuals (S) is at the rate (λ) . This category would be become reduced by the vaccine percentage (ξ) natural death rate and as well as the percentage of the total population getting infected due to contacts with infected individuals and individuals isolated to receive treatment of COVID-19 at these rates of Scores of β_1 , $and\, \beta_2$ respectively.
The Susceptible population are positively proportional to the rate at which recovered individuals are becoming susceptible again, the waning rate of vaccination and the rate at which recovered human population become susceptible again θ_1 , $and\, \theta_2$. The dynamics of the susceptible individuals was consequently defined as;

$$\frac{dS}{dt} = \lambda + \theta_1 V_C + \theta_2 R_C + \theta_3 Q_C - \left(\frac{(\beta_1 I_C + \beta_2 I_{TC})}{N_H} + \xi + \mu \right) S$$

The COVID-19 Exposed people (E_C) grows larger because of the percentage of new cases at the rates $\beta_1,\ and\, \beta_2$. This becomes less because quarantined exposed people become fewer at the rate and as a consequence of the natural death rate (mu), The dynamics of this population is made up as follows;

$$\frac{dE_C}{dt} = \left(\frac{(\beta_1 I_C + \beta_2 I_{TC})}{N_H} \right) S - (\rho_8 + \mu) E_C$$

The number of COVID-19 quarantined individuals (Q_C) increases as exposed individuals move to the quarantine class at the rate of (ρ_8) . This population decreases due to the progression from quarantine to the infected class (ρ_1), and the natural death rate (μ) . The dynamics of this class are formulated as follows.

$$\frac{dQ_C}{dt} = \rho_8 E_C - (\theta_3 + \rho_1 + \mu) Q_C$$

The number of COVID-19 infected individuals (I_C) increases as quarantined individuals progress to the infected class at the rate (ρ_1) . This population decreases due to the natural death rate (μ) , disease-induced death rate (δ_4) , and the rate at which infected individuals are isolated for COVID-19 treatment (α_3). The dynamics of this class are formulated as follows;

$$\frac{dI_C}{dt} = \rho_1 Q_C - (\alpha_3 + \delta_4 + \mu) I_C$$

The number of COVID-19 individuals isolated for treatment (I_{TC}) increases at the rate at which infected individuals are isolated for treatment (α_3) . This population decreases due to recovery from treatment (ϕ_4) , disease-induced death δ_5 , and the natural death rate (μ) .The dynamics of this population are presented as follows.

$$\frac{dI_{TC}}{dt} = \alpha_3 I_C - (\phi_3 + \delta_5 + \mu) I_{TC}$$

The COVID-19 vaccinated population (V_C) increases due to the rate at which susceptible individuals are vaccinated (ξ). This class decreases due to the natural death rate (μ) , the waning rate of the vaccine (θ_1) , and the rate at which recovered individuals become susceptible to the disease again θ_2 . The dynamics of this class are formulated as follows;

$$\frac{dV_C}{dt} = \xi S - (\theta_1 + \mu) V_C$$

The COVID-19 recovered population R_C increases due to the isolation treatment rate (ϕ_4) . This class decreases as recovered individuals become susceptible to the disease again θ_2 and due to the natural death rate (μ) . The dynamics of this class are formulated as follows;

$$\frac{dR_C}{dt} = \phi_4 I_{TC} - (\theta_2 + \mu) R_C$$

The force of infection associated to the population is ;

$$\omega_C = \frac{(\beta_1 I_C + \beta_2 I_{TC})}{N_H}$$

The model flow diagram based on our assumptions is illustrated in Fig. 1.

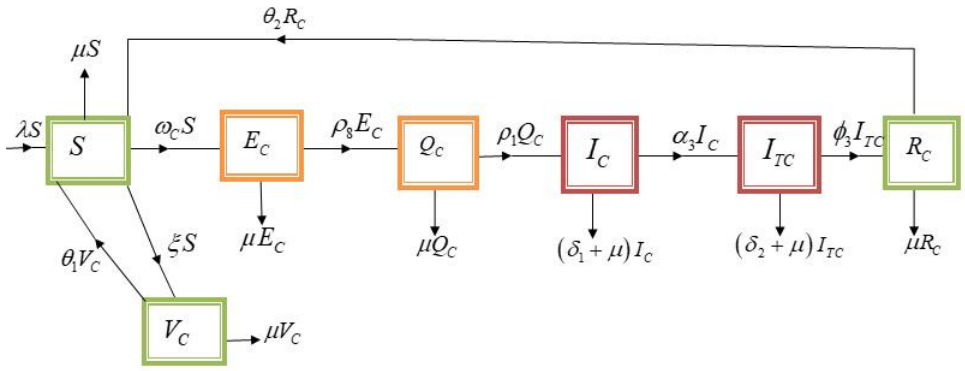

Figure 1: model schematic flow diagram

Similarly, the mathematical model reflecting our assumptions and the aforementioned description is provided as follows:
The total human population is given as:

$$N_H(t) = S(t) + E_C(t) + Q_C(t) + I_C(t) + I_{TC}(t) + V_C(t) + R_C(t)$$

$$\left.\begin{aligned}
\frac{dS}{dt} &= \lambda + \theta_1 V_C + \theta_2 R_C + \theta_3 Q_C - \left(\frac{(\beta_1 I_C + \beta_2 I_{TC})}{N_H} + \xi + \mu\right) S \\
\frac{dE_C}{dt} &= \left(\frac{(\beta_1 I_C + \beta_2 I_{TC})}{N_H}\right) S - (\rho_8 + \mu) E_C \\
\frac{dQ_C}{dt} &= \rho_8 E_C - (\theta_3 + \rho_1 + \mu) Q_C \\
\frac{dI_C}{dt} &= \rho_1 Q_C - (\alpha_3 + \delta_4 + \mu) I_C \\
\frac{dI_{TC}}{dt} &= \alpha_3 I_C - (\phi_3 + \delta_5 + \mu) I_{TC} \\
\frac{dV_C}{dt} &= \xi S - (\theta_1 + \mu) V_C \\
\frac{dR_C}{dt} &= \phi_4 I_{TC} - (\theta_2 + \mu) R_C
\end{aligned}\right\} \tag{5}$$

Where $\omega_H = \frac{(\psi_1 I_{AH} + \psi_2 I_{CR} + \psi_3 T_H)}{N_H}$

2 Fractional COVID-19 mathematical model

Here we generalize the integer-order COVID-19 model shown in Eq.(5) with the use of the Caputo derivation operator of fractional order. The new model as compared to the classical model given by the equation (5) is more flexible because with the fractional-order model one can have varying responses:

$$\left.\begin{aligned}
{}^cD_t^\gamma S &= \lambda + \theta_1 V_C + \theta_2 R_C + \theta_3 Q_C - \omega_C S - K_1 S \\
{}^cD_t^\gamma E_C &= \omega_H S - K_2 E_C \\
{}^cD_t^\gamma Q_C &= \rho_8 E_C - K_3 Q_C \\
{}^cD_t^\gamma I_C &= \rho_1 Q_C - K_4 I_C \\
{}^cD_t^\gamma I_{TC} &= \alpha_3 I_C - K_5 I_{TC} \\
{}^cD_t^\gamma V_C &= \xi S - (\theta_1 + \mu) V_C \\
{}^cD_t^\gamma R_H &= \phi_1 I_{AH} + \phi_2 I_{CR} + \phi_3 T_H - K_5 R_H
\end{aligned}\right\} \tag{6}$$

where

$$K_1 = (\xi+\mu), K_2 = (\rho_8 + \mu), K_3 = (\theta_3 + \rho_1 + \mu), K_4 = (\alpha_3 + \delta_4 + \mu), K_5 = (\phi_4 + \delta_5 + \mu), K_6 = (\theta_1 + \mu), K_7 = \tag{7}$$

Subject to the positive initial conditions

$$S(0) = S_0, \;\; E_C(0) = E_{C0}, \;\; Q_C(0) = Q_{C0}, \;\; I_C(0) = I_{C0}, \;\; I_{TC}(0) = I_{TC0}, V_C(0) = V_{C0}, \;\; R_C(0) = R_{C0} \tag{8}$$

3 Model analysis

3.1. positivity of model solution
We considered the non-negativity of the initial values
$\lim Sup.N_H(t) \leq \frac{\lambda}{\mu}$, Secondly, If $\lim Sup.N_{H0}(t) \leq \frac{\lambda}{\mu}$, then our model feasible domain is given by:

$$\Omega = \left\{(S, E_C, Q_C, I_C, I_{TC}, V_C, R_C) \subset R_+^7 : S + E_C + I_C + I_{TC} + V_C + R_C \leq \frac{\lambda}{\mu},\right\}$$

$\Omega = \Omega_C \subset R_+^7$,
.From Eq. (6), picking the first equation, we have that hence

Ω is positively invariant.
If $S_0, E_{C0}, Q_{C0}, I_{C0}, I_{TC0}, V_{C0} \;\; and \;\; R_{C0}$ are non-negative, then the solution of model (6) will be non-negative for $t > 0$

$${}^cD_t^\gamma S = \lambda + \theta_1 V_C + \theta_2 R_C + \theta_3 Q_C - \omega_C S - K_1 S$$

$${}^{c}D_t^{\gamma} S + \omega_C S + (\xi + \mu) S = \lambda + \theta_1 V_C + \theta_2 R_C + \theta_3 Q_C$$

But $\lambda + \theta_1 V_C + \theta_2 R_C + \theta_3 Q_C \geq 0,\ then,$

$${}^{c}D_t^{\gamma} S + \omega_C S + (\xi + \mu) S \geq 0.$$

Applying the Laplace transform we obtained;

$$L\left[{}^{c}D_t^{\gamma} S\right] + \left[\omega_C S + (\xi + \mu) S\right] \geq 0,$$

$$S^{\gamma} S(s) - S^{\gamma-1} S(0) + (\omega_C + \xi + \mu) S(s) \geq 0,$$

$$S(s) \geq \frac{S^{\gamma-1}}{S^{\gamma} + (\omega_C + \xi + \mu)} S(0).$$

By taking the inverse Laplace transform, we obtained ;

$$S(t) \geq E_{r,1}\left(-(\omega_C + \xi + \mu) t^{\gamma}\right) S_0. \tag{9}$$

Now since the term on the right hand side of Eq. (9) is positive, we conclude that, $S \geq 0$ for $t \geq 0$. In the same way, we also have that , $E_C \geq 0$, $Q_C \geq 0,\ I_C \geq 0,\ I_{TC} \geq 0,\ V_C \geq 0$, $R_C \geq 0$,
that is are positives, therefore, the solution will remain in R_+^7 for all $t \geq 0$ with positive initial conditions.

3.2 Boundedness of fractional model solution.

The total population of individuals from our model is given by ;
$N_H(t) = S(t) + E_C(t) + Q_C(t) + I_C(t) + I_{TC}(t) + V_C(t) + R_C(t)$.
So from our fractional model (6), we now obtain:

$${}^{c}D_t^{\gamma} N_H(t) = {}^{c}D_t^{\gamma} S(t) + {}^{c}D_t^{\gamma} E_C(t) + {}^{c}D_t^{\gamma} Q_C(t) + {}^{c}D_t^{\gamma} I_C(t) + D_t^{\gamma} I_{TC}(t) + {}^{c}D_t^{\gamma} V_C(t) + {}^{c}D_t^{\gamma} R_C(t),,$$

$${}^{c}D_t^{\gamma} N_H(t) = \lambda - \mu N_H(t) \tag{10}$$

Taking the Laplace transformation of (10) we obtained;

$$L\left[{}^{c}D_t^{\gamma} N_H(t)\right] \leq L\left[\lambda - \mu N_H(t)\right],$$

$$S^{\gamma} N_H(s) - S^{\gamma-1} N_H(0) + \mu N_H(s) \leq \frac{\lambda}{\mu},$$

$$N_H(s) \leq \frac{S^{\gamma-1}}{(S^{\gamma} + \mu)} N_H(0) + \frac{\lambda}{S(S^{\gamma} + \mu)} \tag{11}$$

By taking the inverse Laplace transform of Eq. (11) we obtained ;

$$N_H(t) \leq E_{r,1}\left(-\mu t^{\gamma}\right) N_H(0) + \lambda E_{r,r+1}\left(-\mu t^{\gamma}\right) \tag{12}$$

At $t \to \infty$, the limit of Eq. (12) becomes

$$\lim_{t \to \infty} Sup N_H(t) = \frac{\lambda}{\mu}.$$

$N_{H0} \leq \frac{\lambda}{\mu}$ then, $N_H(t) \leq \frac{\lambda}{\mu}$ which means that, $N_H(t)$ is bounded.
We now say that, this region $\Omega = \Omega_H$,is well posed and equally feasible epidemiologically.

3.3 Existence and uniqueness of our model solution

Let the real non-negative be P, we consider
$Q = [0, P]$.

All the continuous functions on M is denoted as: $N_e^0(Q)$ with norm as;

$$\|X\| = Sup\{|X(t)|, t \in Q\}.$$

The model (6) with initial conditions in (8) that can be called as initial value problem (IVP) in (13).

$$^cD_t^\gamma(t) = Z(t, X(t)), \ 0 < t < P < \infty,$$

$$X(0) = X_0. \tag{13}$$

where

$$Y(t) = (S(t), E_C(t), Q_C(t), I_C(t), I_{TC}(t), V_C(t), R_C(t))$$

represents the classes and Z be a continuous function defined as follows;

$$beginarrayZ(t, X(t)) = \begin{pmatrix} Z_1(t, S(t)) \\ Z_2(t, E_C(t)) \\ Z_3(t, Q_C(t)) \\ Z_4(t, I_C(t)) \\ Z_5(t, I_{TC}(t)) \\ Z_6(t, V_C(t)) \\ Z_7(t, R_C(t)) \end{pmatrix} = \begin{pmatrix} \lambda + \theta_1 V_C + \theta_2 R_C + -\left(\frac{\beta_1 I_C + \beta_2 I_{TC}}{N_H}\right) S - (\xi + \mu) S \\ \left(\frac{\beta_1 I_C + \beta_2 I_{TC}}{N_H}\right) S - (\rho_8 + \mu) E_C \\ \rho_8 E_C - (+\rho_1 + \mu) Q_C \\ \rho_1 Q_C - (\alpha_3 + \delta_4 + \mu) I_C \\ \alpha_3 I_C - (\phi_3 + \delta_5 + \mu) I_{TC} \\ \xi S - (\theta_1 + \mu) V_C \\ \phi_4 I_{TC} - (\theta_2 + \mu) R_C \end{pmatrix} \tag{14}$$

Using proposition (2.1), we have that,

$$\begin{aligned} S(t) &= S_0 + I_t^\gamma \left[\lambda + \theta_1 V_C + \theta_2 R_C + -\left(\frac{\beta_1 I_C + \beta_2 I_{TC}}{N_H}\right) S - (\xi + \mu) S.\right], \\ E_C(t) &= E_{C0} + I_t^\gamma \left[\left(\frac{\beta_1 I_C + \beta_2 I_{TC}}{N_H}\right) S - (\rho_8 + \mu) E_C\right], \\ Q_C(t) &= Q_{C0} + I_t^\gamma \left[\rho_8 E_C - (+\rho_1 + \mu) Q_C\right], \\ I_C(t) &= I_{C0} + I_t^\gamma \left[\rho_1 Q_C - (\alpha_3 + \delta_4 + \mu) I_C\right], \\ I_{TC}(t) &= I_{TC0} + I_t^\gamma \left[\alpha_3 I_C - (\phi_3 + \delta_5 + \mu) I_{TC}\right], \\ V_C(t) &= V_{C0} + I_t^\gamma \left[\xi S - (\theta_1 + \mu) V_C\right], \\ R_C(t) &= R_{C0} + I_t^\gamma \left[\phi_4 I_{TC} - (\theta_2 + \mu) R_C\right]. \end{aligned} \tag{15}$$

We obtain the Picard iteration of (15) as follows;

$$
\begin{aligned}
S_n(t) &= S_0 + \frac{1}{\Gamma(\gamma)} \int_0^t (t-\lambda)^{\gamma-1} Z_1(\lambda, S_{n-1}(\lambda))\, d\lambda, \\
E_{Cn}(t) &= E_{C0} + \frac{1}{\Gamma(\gamma)} \int_0^t (t-\lambda)^{\gamma-1} Z_2\left(\lambda, E_{C(n-1)}(\lambda)\right) d\lambda, \\
Q_{Cn}(t) &= Q_{C0} + \frac{1}{\Gamma(\gamma)} \int_0^t (t-\lambda)^{\gamma-1} Z_3\left(\lambda, Q_{C(n-1)}(\lambda)\right) d\lambda, \\
I_{Cn}(t) &= I_{C0} + \frac{1}{\Gamma(\gamma)} \int_0^t (t-\lambda)^{\gamma-1} Z_4\left(\lambda, I_{C(n-1)}(\lambda)\right) d\lambda, \\
I_{TCn}(t) &= I_{TC0} + \frac{1}{\Gamma(\gamma)} \int_0^t (t-\lambda)^{\gamma-1} Z_4\left(\lambda, I_{TC(n-1)}(\lambda)\right) d\lambda, \\
V_{Cn}(t) &= V_{C0} + \frac{1}{\Gamma(\gamma)} \int_0^t (t-\lambda)^{\gamma-1} Z_5\left(\lambda, V_{C(n-1)}(\lambda)\right) d\lambda, \\
R_{Cn}(t) &= R_{C0} + \frac{1}{\Gamma(\gamma)} \int_0^t (t-\lambda)^{\gamma-1} Z_6\left(\lambda, R_{C(n-1)}(\lambda)\right) d\lambda.
\end{aligned} \tag{16}
$$

We now converted the first value problem of Eq. (13) to have:

$$
X(t) = X(0) + \frac{1}{\Gamma(\gamma)} \int_0^t (t-\lambda)^{\gamma-1} Z(\lambda, X(\lambda))\, d\lambda. \tag{17}
$$

Lemma 1, The Lipchitz condition described from Eq. (14) is satisfied by vector $Z(t, X(t))$ on a set $[0, P] \times R_+^7$ with the Lipchitz constant given as;

$\beta = \max\left((\beta_1^* + \beta_2^* + \mu), (\xi + \mu), (\rho_8 + \mu), (+\rho_1 + \mu), (\alpha_3 + \delta_4 + \mu), (\phi_3 + \delta_5 + \mu), (\theta_1 + \mu), (\theta_2 + \mu)\right)$.
Proof.

$\|Z_1(t, S) - Z_1(t, S_1)\|$

$= \left\| \lambda + \theta_1 V_C + \theta_2 R_C + - \left(\frac{\beta_1 I_C + \beta_2 I_{TC} - (\xi+\mu)}{N_H}\right) S - \lambda - \theta_1 V_C - \theta_2 R_C - \theta_3 Q_C - \left(\frac{\beta_1 I_C + \beta_2 I_{TC} - (\xi+\mu)}{N_H}\right) S_1 \right\|,$
$= \left\| - \left(\frac{\beta_1 I_C + \beta_2 I_{TC} - (\xi+\mu)}{N_H}\right)(S - S_1) + \mu(S - S_1) \right\| \leq (\beta_1{}^* + \beta_2{}^*) \|S - S_1\| + \mu \|S - S_1\|,$
therefore,
$\|Z_1(t, S) - Z_1(t, S_1)\| \leq (\beta_1{}^* + \beta_2{}^* + \xi + \mu) \|S - S_1\|.$

Similarly we obtained the following;

$$
\begin{aligned}
&\|Z_2(t, E_C) - Z_2(t, E_{C1})\| \leq (\rho_8 + \mu) \|E_C - E_{C1}\|, \\
&\|Z_3(t, Q_C) - Z_3(t, Q_{C1})\| \leq (+\rho_1 + \mu) \|Q_C - Q_{C1}\|, \\
&\|Z_4(t, I_C) - Z_4(t, I_{C1})\| \leq (\alpha_3 + \delta_4 + \mu) \|I_C - I_{C1}\|, \\
&\|Z_5(t, I_{TC}) - Z_5(t, I_{TC1})\| \leq (\phi_3 + \delta_5 + \mu) \|I_{TC} - I_{TC1}\|, \\
&\|Z_6(t, V_C) - Z_6(t, V_{C1})\| \leq (\theta_1 + \mu) \|V_C - V_{C1}\|, \\
&\|Z_7(t, R_C) - Z_7(t, R_{C1})\| \leq (\theta_2 + \mu) \|R_C - R_{C1}\|.
\end{aligned} \tag{18}
$$

where we obtained

$\|Z(t, X_1(t)) - Z(t, X_2(t))\| \leq \beta \|X_1 - X_2\|,$

$$
\beta = \max\left((\beta_1^* + \beta_2^* + \mu), (\xi + \mu), (\rho_8 + \mu), (+\rho_1 + \mu), (\alpha_3 + \delta_4 + \mu), (\phi_3 + \delta_5 + \mu), (\theta_1 + \mu), (\theta_2 + \mu)\right). \tag{19}
$$

Lemma 2. The initial value problem (6), (7) in Eq. (19) exists and will have a unique solution

$X(t) \in A_c^0(f)$.

Using Picard-Lindelof and fixed point theory, we consider the solution of

$X(t) = S(X(t))$,

where S is defined as the Picard operator expressed as ;

$S : A_c^0\left(f, R_+^7\right) \to A_c^0\left(f, R_+^7\right)$.

Hence,

$S(X(t)) = X(0) + \frac{1}{\Gamma(\gamma)} \int_0^t (t-\lambda)^{\gamma-1} Z(\lambda, X(\lambda))\, d\lambda.$

which becomes,

$\|S(X_1(t)) - S(X_2(t))\|$

$= \left\| \frac{1}{\Gamma(\gamma)} \left[\int_0^t (t-\lambda)^{\gamma-1} Z(\lambda, X_1(\lambda)) - Z(\lambda, X_2(\lambda))\, d\lambda \right] \right\|$

$\leq \frac{1}{\Gamma(\gamma)} \int_0^t (t-\lambda)^{\gamma-1} \|Z(\lambda, X_1(\lambda)) - Z(\lambda, X_2(\lambda))\, d\lambda\|$.

$\leq \frac{\beta}{\Gamma(\gamma)} \int_0^t (t-\lambda)^{\gamma-1} \|X_1 - X_2\|\, d\lambda.$

$\|S(X_1(t)) - S(X_2(t))\| \leq \frac{\beta}{\Gamma(\gamma+1)S}.$

where
$\frac{\beta}{\Gamma(\gamma+1)} S \leq 1$,
then, the Picard operator gives a contradiction , so Eq.(6) , (7) solution is unique.

3.4. The COVID-19 Disease free equilibrium points

Disease free-Equilibrium point is a steady steady state where the population of humans is free of the disease.
Disease free equililbrum point of the model (5) is expressed as:

At DFEP

$$(S^*, E^*, Q_C^*, I_C^*, I_{TC}^*, V_C^*, R_C^*) = \left(\frac{\lambda(\omega_C + \mu)}{\mu(\omega_C + \xi + \mu)}, 0, 0, 0, 0, \frac{\lambda}{\mu(\omega_C + \xi + \mu)}, 0 \right) \quad (20)$$

3.5. The basic reproduction number R_0 of model

Basic Reproduction number of the an infectious disease is the secondary cases of infection when an infectious human is introduce into a susceptible population within the period of his or her infectiousness.

In computing the basic reproduction number, we apply the method used in [11].

Let $n = (E_C, Q_C, I_C, I_{TC})$

So that, $\frac{dn}{dt} = F - V$.

Where

$$F = \begin{bmatrix} 0 & 0 & \frac{\beta_1(\theta_1+\mu)}{(\xi+\theta_1+\mu)} & \frac{\beta_2(\theta_1+\mu)}{(\xi+\theta_1+\mu)} \\ 0 & 0 & 0 & 0 \\ 0 & 0 & 0 & 0 \\ 0 & 0 & 0 & 0 \end{bmatrix}$$

$$V = \begin{bmatrix} K_1 & 0 & 0 & 0 \\ -\rho_8 & K_2 & 0 & 0 \\ 0 & -\rho_1 & K_3 & 0 \\ 0 & 0 & -\alpha_3 & K_4 \end{bmatrix} K_1 = (\rho_8 + \mu), K_2 = (\theta_3 + \rho_1 + \mu), K_3 = (\alpha_3 + \delta_4 + \mu), K_4 = (\phi_4 + \delta_5 + \mu).$$

Mathematically, the basic reproduction number is computed as:

$R_0 = \rho\left(FV^{-1}\right)$, where ρ is the dominant Eigen value of the system

$\left(FV^{-1}\right)$

Where R_0 is the basic reproduction number associated with the individuals in the population.

$$R_0 = \frac{(\theta_1 + \mu)\rho_1\rho_8(\beta_1 K_4 + \beta_2\alpha_3)}{(\xi + \theta_1 + \mu)K_3K_2K_1K_4} \tag{21}$$

Since $K_1 = (\rho_8 + \mu)$, $K_2 = (\rho_1 + \mu)$, $K_3 = (\alpha_3 + \delta_4 + \mu)$, $K_4 = (\phi_4 + \delta_5 + \mu)$.

3.5 Endemic equilibrium point

We also examined a non-zero endemic equilibrium point, a positive steady state in which COVID-19 is permanent in the population. In this equilibrium condition the model has all non-zero variables.

$$(S^* \neq 0, E_C^* \neq 0,\ Q_C^* \neq 0, I_C^* \neq 0\ , I_{TC}^* \neq 0,\ \ R_C^* \neq 0).$$

We solve the model equations with regard to the infection force impacting population to analyse the endemic equilibrium point. Based on the fractional COVID-19 model (6), the endemic equilibrium state would be given by;

defined as;

$$\begin{aligned}
S^{**} &= \frac{\lambda K_1 K_2 K_3 K_4 K_5 K_6}{\left(\left(K_2\left(\omega_C^{**}+\xi+\mu\right)K_1-\omega_C\rho_8\right)K_5-\theta_1 K_1 K_2\xi\right)K_6K_4K_3-\theta_2 K_5\omega_C\rho_8\rho_1\alpha_3\phi_4},\\
E_C^{**} &= \frac{\lambda K_2 K_3 K_4 K_5 K_6 \omega_C^{**}}{\left(\left(K_2\left(\omega_C^{**}+\xi+\mu\right)K_1-\omega_C\rho_8\right)K_5-\theta_1 K_1 K_2\xi\right)K_6K_4K_3-\theta_2 K_5\omega_C^{**}\rho_8\rho_1\alpha_3\phi_4},\\
Q_C^{**} &= \frac{\lambda K_3 K_4 K_5 K_6 \omega_C^{**}\rho_8}{\left(\left(K_2\left(\omega_C^{**}+\xi+\mu\right)K_1-\omega_C^{**}\rho_8\right)K_5-\theta_1 K_1 K_2\xi\right)K_6K_4K_3-\theta_2 K_5\omega_C^{**}\rho_8\rho_1\alpha_3\phi_4},\\
I_C^{**} &= \frac{\lambda K_4 K_5 K_6 \omega_C^{**}\rho_8\rho_1}{\left(\left(K_2\left(\omega_C^{**}+\xi+\mu\right)K_1-\omega_C^{**}\rho_8\right)K_5-\theta_1 K_1 K_2\xi\right)K_6K_4K_3-\theta_2 K_5\omega_C^{**}\rho_8\rho_1\alpha_3\phi_4},\\
I_{TC}^{**} &= \frac{\lambda K_5 K_6 \omega_C^{**}\rho_8\rho_1\alpha_3}{\left(\left(K_2\left(\omega_C^{**}+\xi+\mu\right)K_1-\omega_C^{**}\rho_8\right)K_5-\theta_1 K_1 K_2\xi\right)K_6K_4K_3-\theta_2 K_5\omega_C^{**}\rho_8\rho_1\alpha_3\phi_4},\\
V_C^{**} &= \frac{\xi\lambda K_3 K_4 K_6 K_1 K_2}{\left(\left(\left(\omega_C^{**}+\xi+\mu\right)K_5-\theta_1\xi\right)K_2K_1-K_5\omega_C^{**}\rho_8\right)K_6K_4K_3-\theta_2 K_5\omega_C^{**}\rho_8\rho_1\alpha_3\phi_4},\\
R_C^{**} &= \frac{\phi_4\alpha_3\rho_1\rho_8\omega_C^{**}K_5\lambda}{\left(\left(K_2\left(\omega_C^{**}+\xi+\mu\right)K_1-\omega_C^{**}\rho_8\right)K_5-\theta_1 K_1 K_2\xi\right)K_6K_4K_3-\theta_2 K_5\omega_C^{**}\rho_8\rho_1\alpha_3\phi_4}.
\end{aligned} \tag{22}$$

Incorporating in the force of infection in the COVID 19 model into the endemic equilibrium point,

$$\omega_C^{**} = \frac{\beta_1 I_C + \beta_2 I_{TC}}{N_H} \tag{23}$$

we obtained;

$$Q_1\omega_C^{**} + Q_2 = 0 \tag{24}$$

$$Q_1 = K_2K_3K_4K_5K_6 + K_3K_4K_5K_6\rho_8 + K_4K_5K_6\rho_1\rho_8 + K_5K_6\alpha_3\rho_1\rho_8 + K_5\alpha_3\phi_4\rho_1\rho_8 \tag{25}$$

$$Q_2 = \xi K_1K_2K_3K_4K_5K_6 + K_5K_6\rho_1\rho_8\left(1-\frac{K_4\beta_1+\alpha_3\rho_1\beta_2}{K_1K_2K_3K_4}\right) \tag{26}$$

$$Q_2 = \xi K_1K_2K_3K_4K_5K_6 + K_5K_6\rho_1\rho_8\left(1-R_0^C\right) \tag{27}$$

Where
$K_1 = (\rho_8+\mu)\,,\ K_2 = (\rho_1+\mu)\,,\ K_3 = (\alpha_3+\delta_4+\mu)\,,\ K_4 = (\phi_4+\delta_5+\mu)\,.$

From above we observed that for ω_C^{**} then $R_0 > 1$ Which implies that, the endemic equilibrium point of model (6) is stable.

3.6. Global stability analysis at endemic equilibrium state

To analyse global stability, the equilibrium point is treated with direct Lyapunov method. In the case when $R_0 > 1$ the endemic equilibrium point is globally stable. Epidemiological implication of the same is that the disease will spread throughout the entire population with or without the initial prerequisites. As it can be seen in fractional model (6).

$\omega_C = \frac{\beta_1 I_C}{N_H} + \frac{\beta_2 I_{TC}}{N_H}$

Where

$N_H \leq \frac{\lambda}{\mu}\ as\ t \to \infty$
then,

$\omega_C = \beta_1 I_C + \beta_2 I_{TC}$

our fractional model now becomes;

$$\left.\begin{array}{c} {}^cD_t^\gamma S = \lambda + \theta_1 V_C + \theta_2 R_H + \theta_3 Q_C - \omega_{C1} S - K_1 S \\ {}^cD_t^\gamma E_C = \omega_{C1} S - K_2 E_C, \\ {}^cD_t^\gamma Q_C = \rho_C E_C - K_3 Q_C, \\ {}^cD_t^\gamma I_C = \rho_1 Q_C - K_4 I_C \\ {}^cD_t^\gamma I_{TC} = \alpha_3 I_C - K_5 I_{TC} \\ {}^cD_t^\gamma V_C = \xi S - K_6 V_C \\ {}^cD_t^\gamma R_C = \phi_4 I_{TC} - K_7 R_C. \end{array}\right\} \tag{28}$$

At equilibrium point Eq. (24) has the following results:

$\lambda = \omega_{C1}^* S^* + K_1 S^* - \theta_1 V_C^* - \theta_2 R_C^* - \theta_3 Q_C^*$, $K_2 E_C^* = \omega_{C1}^* S^*$,
$K_3 Q_C^* = \rho_8 E_C^*$,$K_4 I_C^* = \rho_1 Q_C^*$,
$K_5 I_{TC}^* = \alpha_3 I_C^*$,$K_6 V_C^* = \xi S^*$,
$K_7 R_C^* = \phi_4 I_{TC}^*$.

Theorem 1. Model (24) is globally asymptotically stable if $R_0 > 1$, whenever

$\left(7 - \frac{S^*}{S} + \frac{\omega_{C1}}{\omega_{C1}^*}\left(1 - \frac{S E_C^*}{S^* E_C}\right) - \frac{I_C^* E_C Q_C}{I_C E_C^* Q_C} - \frac{I_{TC}}{I_{TC}^*} - \frac{I_{TC}^* I_C}{I_{TC} I_C^*}\right) \leq 0.$

Let $L(t) = L_C(t)$ be a non-linear Lyaponov function as presented in (25) below:

$$\begin{array}{l} L(t) = L_1\left(S - S^* - S^* \ln \frac{S}{S^*}\right) + L_2\left(E_C - E_C^* - E_C^* \ln \frac{E_C}{E_C^*}\right) + L_3\left(Q_C - Q_C^* - Q_C^* \ln \frac{Q_C}{Q_C^*}\right) \\ + L_4\left(I_C - I_C^* - I_C^* \ln \frac{I_C}{I_C^*}\right) + L_5\left(I_{TC} - I_{TC}^* - I_{TC}^* \ln \frac{I_{TC}}{I_{TC}^*}\right) + L_6\left(V_C - V_C^* - V_C^* \ln \frac{V_C}{V_C^*}\right) \\ + L_7\left(R_C - R_C^* - R_C^* \ln \frac{R_C}{R_C^*}\right). \end{array} \tag{29}$$

With Caputo Fractional order, derivative as to Eq (25), we get:

$$
\begin{aligned}
{}^cD_t^\gamma L(t) = {}^cD_t^\gamma L_H(t) \le L_1\left(1-\tfrac{S^*}{S}\right){}^cD_t^\gamma S(t) + L_2\left(1-\tfrac{E_C^*}{E_C}\right)^c D_t^\gamma E_C(t) \\
+L_3\left(1-\tfrac{Q_C^*}{I_{AH}}\right)^c D_t^\gamma Q_C(t) + L_4\left(1-\tfrac{I_C^*}{I_C}\right)^c D_t^\gamma I_C(t) + L_5\left(1-\tfrac{I_{TC}^*}{I_{TC}}\right)^c D_t^\gamma I_{TC} \\
(t) + L_6\left(1-\tfrac{V_C^*}{V_C}\right)^c D_t^\gamma V_C(t) + L_7\left(1-\tfrac{R_C^*}{R_C}\right)^c D_t^\gamma R_C(t).
\end{aligned}
$$

$$
= \omega_{C1}^* S^* \begin{pmatrix} \left(1-\tfrac{S^*}{S}\right)^c D_t^\gamma S(t) + \left(1-\tfrac{E_C^*}{E_C}\right)^c D_t^\gamma E_C(t) \\ +\left(1-\tfrac{Q_C^{**}}{Q_C}\right)^c D_t^\gamma Q_C(t) + \left(1-\tfrac{I_C^*}{I_C}\right)^c D_t^\gamma I_C(t) \\ +\left(1-\tfrac{I_{TC}^*}{I_{TC}}\right)^c D_t^\gamma I_{TC}(t) + \left(1-\tfrac{V_C^*}{V_C}\right)^c D_t^\gamma I_{TC}(t) \\ +\left(1-\tfrac{R_C^*}{R_C}\right)^c D_t^\gamma R_C(t) \end{pmatrix}.
$$

$$
\left(1-\frac{S^*}{S}\right)^c D_t^\gamma S = \left(1-\frac{S^*}{S}\right)\begin{pmatrix} \omega_{C1}^* S^* + K_1 S^* - \theta_1 V_C \\ -\theta_2 R_C - \theta_3 Q_C - \omega_{C1} S \\ -K_1 S + \theta_1 V_C \end{pmatrix},
$$

$$
\begin{aligned}
= \omega_{C1}^* S^*\left(1-\tfrac{S\omega_{C1}}{\omega_{C1}^* S^*} - \tfrac{S^*}{S} + \tfrac{\omega_{C1}}{\omega_{C1}^*}\right) \\
+K_1 S^*\left(2-\tfrac{S}{S^*}-\tfrac{S^*}{S}\right) - \theta_1 V_C^*\left(1-\tfrac{V_C}{V_C^*}\right)\left(1-\tfrac{S^*}{S}\right),
\end{aligned}
$$

$$
= \omega_{C1}^* S^*\left(1-\frac{S\omega_{C1}}{\omega_{C1}^* S^*} - \frac{S^*}{S} + \frac{\omega_{C1}}{\omega_{C1}^*}\right) + K_1 S^*\left(2-\frac{S}{S^*}-\frac{S^*}{S}\right) - \theta_1 V_C^*\left(1-\frac{V_C}{V_C^*}\right)\left(1-\frac{S^*}{S}\right),
$$

$$
\left(1-\frac{E_C^*}{E_C}\right){}^cD_t^\gamma E_C = \left(1-\frac{E_C^*}{E_C}\right)\left(\omega_{C1}^* S - \omega_{C1}^* S^* \frac{E_C}{E_C^*}\right),
$$

$$
= \omega_{C1}^{**} S^{**}\left(1-\frac{S\omega_{C1}}{\omega_{C1}^* S^*}\frac{E_C^*}{E_C} - \frac{E_C^*}{E_C} + \frac{S\omega_{C1}}{\omega_{C1}^* S^*}\right),
$$

$$
\frac{K_2}{\rho_8}\left(1-\frac{Q_C^*}{I_{AH}Q_C}\right){}^cD_t^\gamma Q_C = \frac{K_2}{\rho_8}\left(1-\frac{Q_C^*}{Q_C}\right)\left(\rho_1 E_C - K_3\frac{Q_C}{Q_C^*}Q_C^*\right),
$$

$$
= \omega_{C1}^* S^*\left(1+\frac{E_C}{E_C^*} - \frac{Q_C}{Q_C^*} - \frac{E_C Q_C^*}{E_C^* Q_C}\right),
$$

$$
\frac{K_3}{\rho_1}\left(1-\frac{I_C^*}{I_C}\right){}^cD_t^\gamma I_C = \frac{K_3}{\rho_1}\left(1-\frac{I_C^*}{I_C}\right)\left(\rho_1 Q_C - K_4\frac{I_C}{I_C^*}I_C^*\right),
$$

$$
= \omega_{C1}^* S^*\left(1-\frac{Q_C}{Q_C^*} - \frac{I_C}{I_C^*} - \frac{Q_C}{Q_C^*}\frac{I_C^*}{I_C}\right),
$$

$$
\frac{K_2 K_3}{\alpha_3\rho_8}\left(1-\frac{I_{TC}^*}{I_{TC}}\right){}^cD_t^\gamma I_{TC} = \frac{K_2 K_3}{\alpha_3\rho_8}\left(1-\frac{I_{TC}^*}{I_{TC}}\right)\left(\frac{I_C}{I_C^*} - \frac{I_{TC}}{I_{TC}^*}\right),
$$

$$
= \omega_{C1}^* S^*\left(1-\frac{I_{TC}}{I_{TC}^*} - \frac{I_C I_{TC}^*}{I_C^* I_{TC}} + \frac{I_C}{I_C^*}\right).
$$

$$
\frac{K_1}{\xi}\left(1-\frac{V_C^*}{V_C}\right){}^cD_t^\gamma V_C = \left(1-\frac{V_C^*}{V_C}\right)\left(\xi S - K_6 V_C^*\frac{V_C}{V_C^*}\right),
$$

$$
= K_1 S^*\left(1-\frac{S}{S^*} - \frac{V_C}{V_C^*} + \frac{V_C^* S}{V_C S^*}\right). \tag{30}
$$

Hence, Eq. (26) now becomes;

$$
\begin{aligned}
&{}^cD_t^\gamma L(t) \le \omega_{C1}^* S^* \\
&\left(7 - \tfrac{S^*}{S} + \tfrac{\omega_{C1}}{\omega_{C1}^*}\left(1-\tfrac{SE_C^*}{S^* E_C}\right) - \tfrac{I_C^* E_C}{I_C E_C^*} - \tfrac{I_{TC}^*}{I_{TC}} - \tfrac{I_{TC}^* I_C}{I_{TC} I_C}\right) \\
&-K_1 S^* \omega_{C1} S^*\left(\left(\tfrac{S^*}{S} - 1 - \ln\tfrac{S^*}{S}\right) + \left(\tfrac{V_C}{V_C^*} - 1 - \ln\tfrac{V_C}{V_C^*}\right) + \left(\tfrac{SV_C^*}{S^* V_C} - 1 - \ln\tfrac{SV_C^*}{S^* V_C^*}\right)\right)
\end{aligned}
$$

$-\theta_1 V_C^* S^* \omega_{C1} S^* \left(1 - \frac{V_C}{V_C^*}\right)\left(1 - \frac{S_*}{S}\right),$

Which implies that,

$${}^cD_t^\gamma L(t) \leq \omega_{C1}^* S^* \beta (R_0 - 1)\lambda S^*$$

$$\left(7 - \frac{S^*}{S} + \frac{\omega_{C1}}{\omega_{C1}^*}\left(1 - \frac{SE_C^*}{S^* E_C}\right) - \frac{I_C^* E_C Q_C}{I_C E_C^* Q_C} - \frac{I_{TC}}{I_{TC}^*} - \frac{I_{TC}^* I_C}{I_{TC} I_C^*}\right) \leq 0.$$

$$-\beta (R_0 - 1)\lambda S^* \left[\begin{array}{l} K_1 S^* \left(\frac{S^*}{S} - 1 - \ln \frac{S^*}{S}\right) + \left(\frac{V_C}{V_C^{**}} - 1 - \ln \frac{V_C^*}{V_C}\right) + \left(\frac{SV_C^*}{S^* V_C} - 1 - \ln \frac{SV_C^*}{S^* V_C}\right) \\ +\theta_1 V_C^* \left(1 - \frac{V_C}{V_C^*}\right)\left(\frac{S^*}{S}\right) \end{array}\right]. \tag{31}$$

Therefore, ${}^cD_t^\gamma L(t) \leq 0 \ \ for \ R_0 > 1.$
This implies that,

$${}^cD_t^\gamma L(t) = 0$$

If $E_* = (S^*, E_C^*,\ Q_C^*,\ I_C^*, I_{TC}^*\ ,\ V_C^*,\ R_C^*)$,

The endemic equilibrium point is the globally asymptotically stable point in Ω
if and only if $R_0 > 1$. by LaSalle invariance principle.

4. 0 Fractional order model numerical results

We numerically solved the fractional-order COVID-19 model by generalized fractional AdamsBashforthMoulton methods suggested in [5]. Table 1 shows the values of the parameters of the model and using that, the model was simulated with varying values of the fractional-order. (γ) has been simulated and taken into consideration.

4 Implementation of fractional Adams-Bashforth-Moulton method

It used the techniques outlined by Baskonus et al.[12], Diethelm[13] and Freed in Diethelm[13]. The numerical approximation of the solution of the fractional COVID-19 model by (6) was carried out with the fractional AdamsBashfort-Moulton method. The fractional model (6) model is portrayed in the following way:

$${}^cD_t^\gamma M(t) = N(t, m(t)),\ 0 < t < \psi, \tag{32}$$

$M^{(n)}(0) = M_0^{(n)},\ \ n = 1, 0,\ ..., m, m = [\gamma]$.
where

$M = \left(S^*, E_C^*, {Q_C}^*, {I_C}^*, I_{TC}^*, V_C^*, R_C^*\right) \in R_+^7$ is a real valued function that is continuous.

Eq. (27) can be therefore be represented using the concept of fractional integral as follows;

$$M(t) = \sum_{n=0}^{m-1} M_0^{(n)} \frac{t^n}{n!} + \frac{1}{\Gamma(\gamma)} \int_0^t (t - y)^{\gamma - 1} R(y, m(y))\, dy \tag{33}$$

Using the method described in [43], we let the step size $g = \frac{\psi}{N},\ N \in \mathrm{N}$
with a grid that is uniform on $[0, \psi]$.

where $t_c = cr,\ c = 0, 1, 1, \ldots N$.
Therefore, the fractional order model of COVID-19 model presented in (6) can be approximated as:

$$
\begin{aligned}
S_{k+1}(t) &= S_0 + \tfrac{g^\gamma}{\Gamma(\gamma+2)}\left\{\lambda - (\beta_1 I_C^n + \beta_2 I_{TC}^n)\tfrac{S^n}{N_H^n} - K_1 S^n + \theta_1 V_C^n + \theta_2 R_C^n + \theta_3 Q_C^n\right\} + \\
&\tfrac{g^\gamma}{\Gamma(\gamma+2)}\sum_{y=0}^{k} dy, k+1\left\{\lambda - (\beta_1 I_{Cy} + \beta_2 I_{TCy})\tfrac{S_y}{N_{Hy}} - K_1 S_y + \theta_1 V_{Cy} + \theta_2 R_{Cy} + \theta_3 Q_{Cy}\right\} \\
E_{Ck+1}(t) &= E_{C0} + \tfrac{g^\gamma}{\Gamma(\gamma+2)}\left\{(\beta_1 I_C^n + \beta_2 I_{TC}^n)\tfrac{S^n}{N_H^n} - K_2 E_C^n\right\} + \\
&\tfrac{g^\gamma}{\Gamma(\gamma+2)}\sum_{y=0}^{k} dy, k+1\left\{(\beta_1 I_C^n + \beta_2 I_{TC}^n)\tfrac{S_y}{N_{Hy}} - K_1 E_{Cy}\right\}, \\
Q_{Ck+1}(t) &= Q_{C0} + \tfrac{g^\gamma}{\Gamma(\gamma+2)}\{\rho_8 E_C^n - K_3 I_C^n\} + \\
&\tfrac{g^\gamma}{\Gamma(\gamma+2)}\sum_{y=0}^{k} dy, k+1\{\rho_8 E_{Cy} - K_3 I_C\}, \\
I_{Ck+1}(t) &= I_{C0} + \tfrac{g^\gamma}{\Gamma(\gamma+2)}\{\rho_1 Q_C^n - K_4 I_C^n\} + \\
&\tfrac{g^\gamma}{\Gamma(\gamma+2)}\sum_{y=0}^{k} dy, k+1\{\rho_1 Q_{Cy} - K_4 I_{Cy}\}, \\
I_{TCk+1}(t) &= I_{TC0} + \tfrac{g^\gamma}{\Gamma(\gamma+2)}\{\alpha_3 I_C^n - K_4 I_{TC}^n\} + \\
&\tfrac{g^\gamma}{\Gamma(\gamma+2)}\sum_{y=0}^{k} dy, k+1\{\alpha_3 I_{Cy} - K_5 I_{TCy}\}, \\
V_{Ck+1}(t) &= RV_{C0} + \tfrac{g^\gamma}{\Gamma(\gamma+2)}\{\xi S^n - K_6 V_C^n\} + \\
&\tfrac{g^\gamma}{\Gamma(\gamma+2)}\sum_{y=0}^{k} dy, k+1\{\xi S_y - K_6 V_{Cy}\}. \\
R_{Ck+1}(t) &= R_{C0} + \tfrac{g^\gamma}{\Gamma(\gamma+2)}\{\phi_4 I_{TC}^n - K_7 R_C^n\} + \\
&\tfrac{g^\gamma}{\Gamma(\gamma+2)}\sum_{y=0}^{k} dy, k+1\{\phi_4 I_{TCy} - K_7 R_{Cy}\}.
\end{aligned}
\tag{34}
$$

where

$$
\begin{aligned}
S_{k+1}(t) &= S_0 + \frac{1}{\Gamma(\gamma)}\sum_{y=0}^{k} f_{y,k+1}\left\{\lambda - (\beta_1 I_{Cy} + \beta_2 I_{TCy})\frac{S_y}{N_{Hy}} - K_1 S_y + \theta_1 V_{Cy} + \theta_2 R_{Cy} + \theta_3 Q_{Cy}\right\}, \\
E_{Ck+1}^n(t) &= E_{C0} + \frac{1}{\Gamma(\gamma)}\sum_{y=0}^{k} f_{y,k+1}\left\{(\beta_1 I_{Cy} + \beta_2 I_{TCy})\frac{S_y}{N_{Hy}} - K_2 E_{Cy}\right\}, \\
Q_{Ck+1}^n(t) &= Q_{C0} + \frac{1}{\Gamma(\gamma)}\sum_{y=0}^{k} f_{y,k+1}\{\rho_8 E_{Cy} - K_3 I_{Cy}\}, \\
I_{Ck+1}^n(t) &= I_{C0} + \frac{1}{\Gamma(\gamma)}\sum_{y=0}^{k} f_{y,k+1}\{\rho_1 Q_{Cy} - K_4 I_{Cy}\}, \\
I_{TCk+1}^n(t) &= I_{TC0} + \frac{1}{\Gamma(\gamma)}\sum_{y=0}^{k} f_{y,k+1}\{\alpha_3 I_{Cy} - K_5 I_{TCy}\}, \\
V_{Ck+1}^n(t) &= V_{C0} + \frac{1}{\Gamma(\gamma)}\sum_{y=0}^{k} f_{y,k+1}\{\xi S_y - K_6 V_{Cy}\}, \\
R_{Ck+1}^n(t) &= R_{C0} + \frac{1}{\Gamma(\gamma)}\sum_{y=0}^{k} f_{y,k+1}\{\phi_4 I_{TCy} - K_7 R_{Cy}\}.
\end{aligned}
\tag{35}
$$

From (29) and (30) obtained;

$$dy_{,K+1} = K^{\gamma+1} - (k-\gamma)\,(k+\gamma)^{\gamma},\ y = 0$$

$$(k-y+2)^{\gamma+1} + (k-\gamma)^{\gamma+1} - 2(k-y+1)^{\gamma+1},\ 1 \le y \le k$$

$$1, y = k+1$$

and

$$f_{y,k+1} = \frac{g^{\gamma}}{\gamma}\left[(k-y+1)^{\gamma}(k-y)^{\gamma}\right],\ 0 \le y \le k.$$

Table 1

Parameters values used for model simulation

4.2. Importance of using the fractional Adam-Bashforth Moulton method in obtaining the numerical solutions of the model

- One extra evaluation of a function per step is sufficient to implement a fractional Adams-Bashforth-Moulton scheme, and high-order accuracy may be achieved.
- This method provides automatic error control and is widely utilized in packaged ODE solvers.
- It can find use in most areas of study such as Engineering, Chemistry including Medicine and thus, it can be regarded as one of the tools that can be beneficial in the solving of partial and fractional-order differential equations.

4.2 Parameters and variables descriptions

Variables	Description	Value/day	Source
λ	Recruitment rate of individuals into the susceptible class	0.029	[4]
β_1	Contact rate between susceptible and infected individuals	0.9999	Fitted
β_2	Contact rate between susceptible and individuals on treatment	0.8328	Fitted
θ_1	waning rate of vaccine	0.0777	Fitted
θ_2	Rate at which recovered individuals become susceptible again	0.0382	Estimated
ϵ	Vaccination rate	0.5521	Fitted
μ	Natural death rate	0.000303	[4]
ρ_8	Rate at which Exposed individuals are quarantined	0.1345	Fitted
ρ_1	Progression Rate from quarantined population to infected population	0.31	Estimated
δ_5	Disease induced death rate of isolated for treatment individuals with infected COVID-19	0.3	Estimated
δ_1	Disease induced death rate of infected individuals with infected COVID-19	0.0200	Estimated
α_3	Isolated for treatment rate of treatment individuals with COVID-19	0.256	Estimated
ϕ_4	Recovery rate of isolated for treatment individuals	0.079	Estimated

Table 1: Parameters values used for the simulations

4.3 The fractional Adam-Bashforth Moulton approach is crucial for obtaining the model's numerical solutions

- The fractional Adam–Bashforth Moulton method attains high-order accuracy with just one extra function evaluation every step.
- This method is a helpful tool for numerical solutions of partial and fractional order differential equations and has potential applications in many fields, including engineering, chemistry, and medicine.
- The Adam–Bashforth Moulton method, which is frequently included in packaged ODE solvers, provides automatic error management.

4.4. Fractional order COVID-19 model simulation

In this section, we present the graphs obtained from numerical simulation of the fractional order COVID-19.

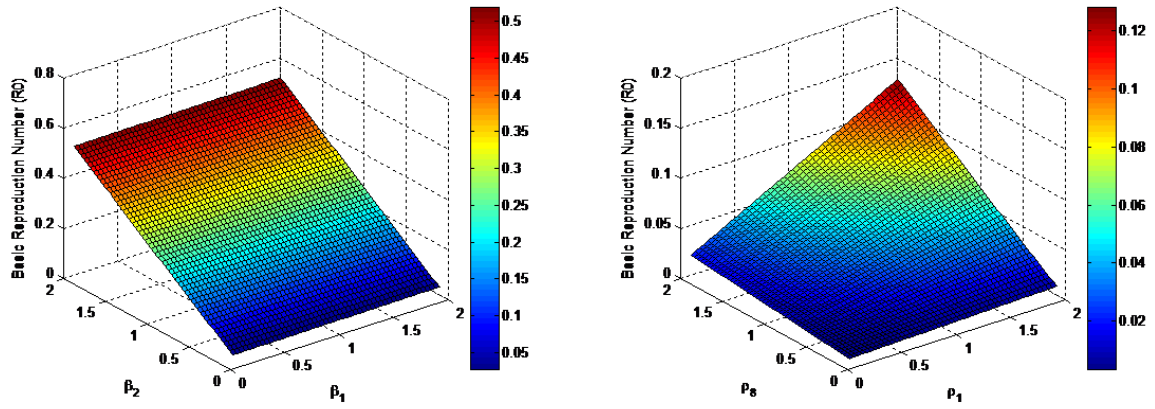

(a) Surface showing the Impact of β_1 and β_1 on $R_0^C C$ (b) Surface showing the Impact of ρ_1 and ρ_8 on R_0^C

Figure 2: surface plot of the basic reproduction number

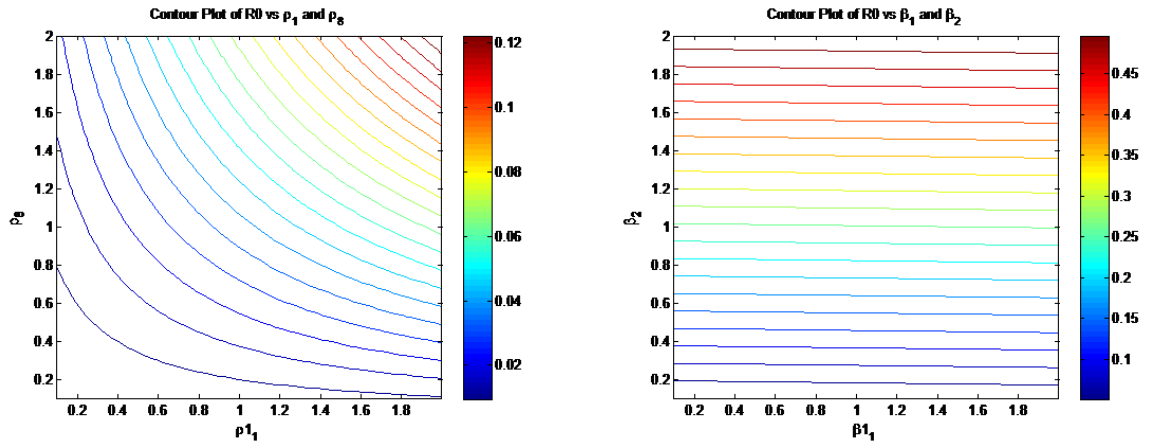

(a) contour plot showing the Impact of ρ_1 and ρ_8 on R_0^C (b) contour plot showing the Impact of β_1 and β_2 on R_0^C

Figure 3: Contour plot on Impact of ρ_1 and ρ_8 on R_0^C and Effect of β_1 and β_2 on R_0^C

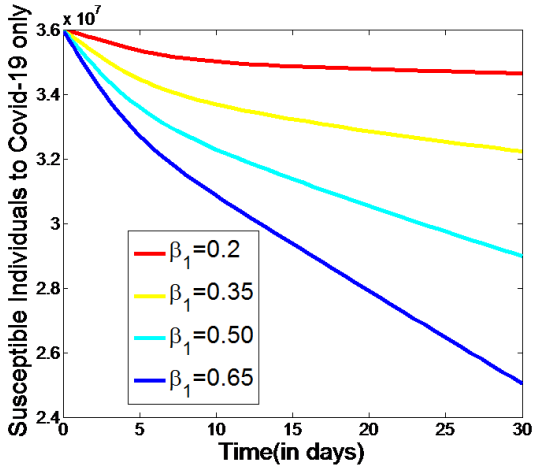

(a) Simulation of Susceptible individuals to COVID-19

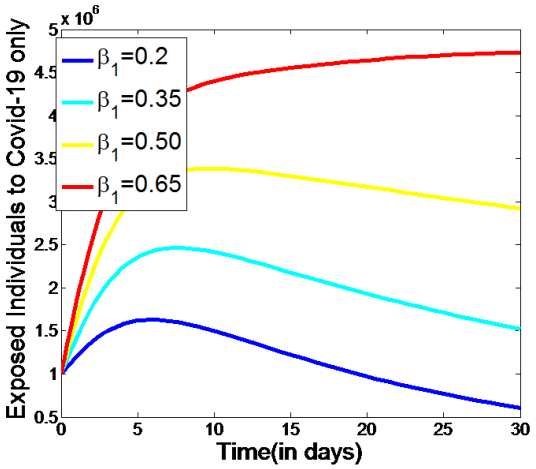

(b) Simulation of Exposed individuals to COVID-19

Figure 4: Effect of β_1 on $S(t)$ and $E_C(t)$

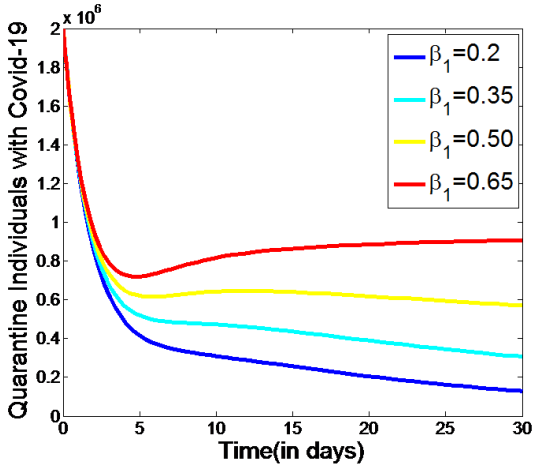

(a) Simulation of Quarantined individuals of COVID-19

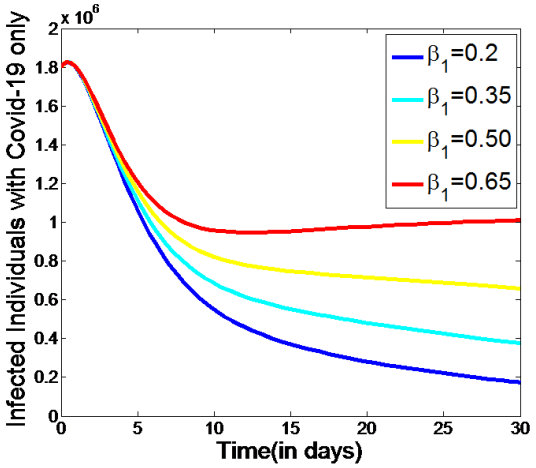

(b) Simulation of infected individuals with COVID-19

Figure 5: Effect of β_1 on $Q_C(t)$ and $I_C(t)$

As indicated by (2a) it will be noted that basic reproductive number $R_0^C(t)$ approaches a maximum less than one (1) as its beta values β_1 and β_2 reduces. It means that the decrease of these parameters will eventually lead to alleviating the influence of COVID-19 on the population. It is seen (2b), that the basic reproduction number $R_0^C(t)$ is highest (although less than one (1)) when ρ_1 and ρ_8 is lower. This shows that by decreasing these parameters, the effect of the COVID-19 will eventually strain the population less. As shown in (3a), the contour plot of in regards to is plotted. On scrutinizing of the numerical flows in the graph, it emerges that the peak score hit was 0.6 when we varied the parameters viz., 0.4, the parameters is also less than one (1). This revelation indicates that increasing these parameters would not cause a noticeable spread of COVID-19 among the population. In addition, the burdens of the COVID-19 virus among the populace can be reduced by increasing the values of ρ_1 and ρ_8 , which represents the treatment rates of acute and chronic infected population respectively. Figure (3b) has the contour plot of with regards to . After observing the numerical streams in the graph, it confirms that the highest value of reached using these parameters, ρ_1 and ρ_8 when

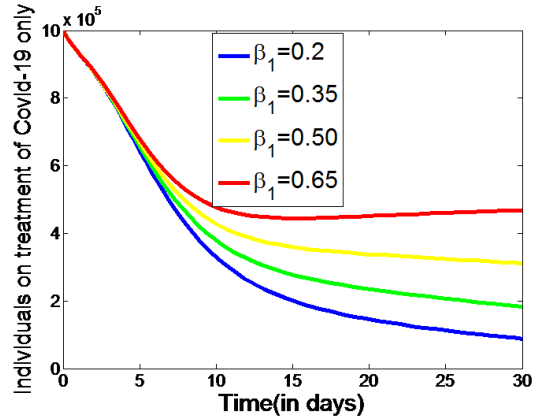

(a) Simulation of individuals isolated for treatment of COVID-19

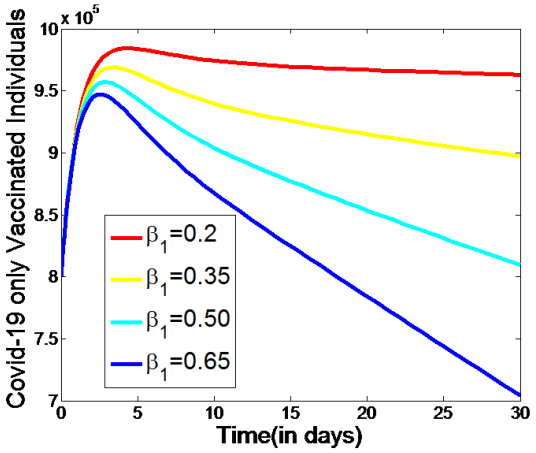

(b) Vaccinated population against COVID-19

Figure 6: Effect of β_1 on $I_T(t)$ and $V_C(t)$

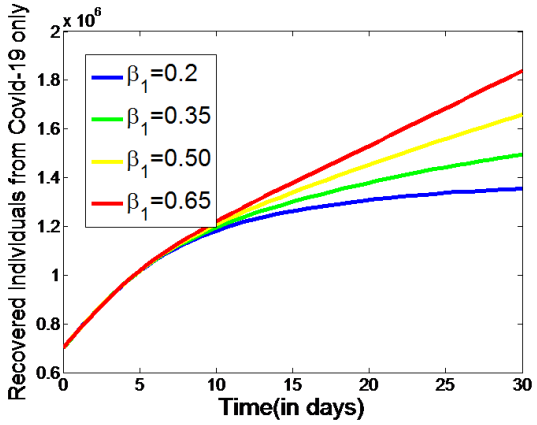

(a) Simulation of Recovered individuals from COVID-19

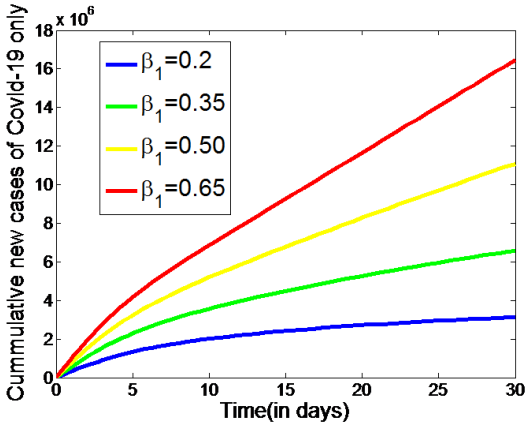

(b) Cumulative New Cases of COVID-19

Figure 7: Effect of β_1 on $R_C(t)$ and $R_0^C(t)$

varied is 0.6 which is less than the value of unity (1). This implies that adding these parameters would not cause a severe breakout of the COVID-19 in the community. Besides, increasing the levels of ρ_1 and ρ_8 defined by treatment proportions of infected individuals with COVID-19 infected and isolated human population respectively, would reduce the COVID-19 burden among the population. The simulation of the influence of the rate of contact of the individuals being infected β_1 by Covid-19 in the individuals only susceptible to Covid-19 are displayed in (4a). It has been noted that, since the only increase leading to the raising of contact rate of individuals infected β_1 with Covid-19 is done, the remaining people susceptible to Covid-19 will decrease. Also, in case we raise the contact rate β_1 of individuals infected with Covid-19 to 20% the population susceptible to Covid-19 will decline to 36000000 within 30 days. It is noted that with the increase in contact rate β 1 of individuals infected with Covid-19 only, the number of Exposed individuals to Covid-19 will be on the rise. Also, when we augment the exposure rate of people with Covid-19 to 20% the Exposed individuals infected with Covid-19 will rise up to 4500000 in 30 days. The simulation of the influence of the contact rate of the Covid-19 infected people to the Quarantined people of Covid-19 is expressed in (5a) It has been noted that the more the contact rate, β_1 of individuals with Covid-19 increases, the more the Quarantined Covid-19 cases will be. Furthermore, when we enhance the contact rate β_1 of

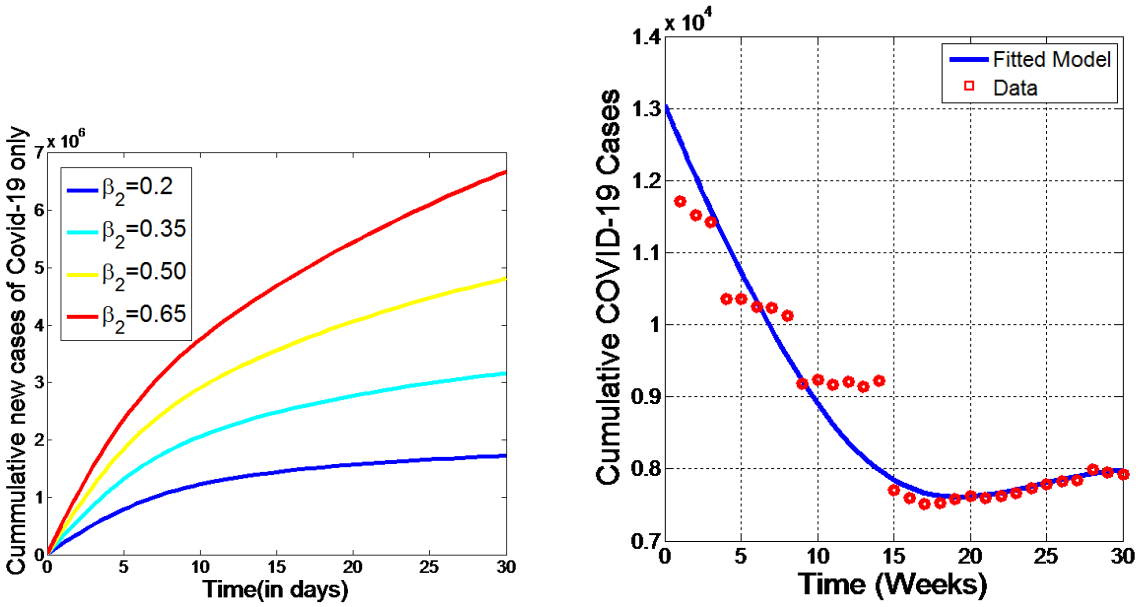

(a) Cummulative new cases of COVID-19 (b) COVID-19 Data Fitting

Figure 8: Effect of β_2 on $R_0^C(t)$ and COVID-19 Data Fitting

persons infected with Covid-19 to only 35% the Quarantined persons infected with Covid-19 will only be below 600000 in a span of 30 days. In (5b), the simulation of the projecting the effect of rate of susceptibility people infected with Covid-19 and others possessing Covid-19 only was represented. It is observed that as the rate of contact (contact rate β_1) of the people infected with Covid-19 increases, the same will increase those who are under COVID 19 care. And when we reduce the frequency with which people are in contact with the Covid-19 virus to 65 percent only, we will not see more than 600 000 people infected with Covid-19 in 30 days. The (6a) are the simulation of the effect of the rate of contact of the subjects infected by the Covid-19 on the plus only Recovered by Covid-19. It is indicated that, an escalation in the rate of contact that persons who have been infected by Covid-19 will only cause a decline in the number of Recovered persons infected by Covid-19. Figure (6b) indicates the simulation of the effect of the rate of contact of individual with Covid-19 on the number of cumulative new cases of Covid-19 (figure number). It is observed that, the greater the magnitude of the competition rate β of individuals subjected to the Covid-19 illness, the greater the number of new Covid-19 instances will pile up. Moreover, as the value of the contact rate β_1 of the infected individuals with Covid-19 is raised to only 65% of the cumulative number of new cases Covid-19 will reach below 16000000 only in 30 days. The figure (7a) represent the simulation of the influence of the contact rate β_2 of individuals infected with Covid-19 on the cumulative new cases of Covid-19. It is noted that with increased Covid-19 contact rate of the people infected with Covid-19 the cumulative death of Covid-19 increases. Also, in case we multiply the rate of contact between individuals with Covid-19 to 65 percent the cumulative new cases of Covid-19 will rise to less than 6000000 within 30 days.

5 Conclusion

The mathematical model of the presented manuscript has to do with the concept of: Caputo-transmission dynamics and control of Covid-19. We are now aware of the importance of fractional modeling. It started with an exhaustive theoretical analysis of the fractional The Covid-19 model which includes aspects like the existence of solution. uniqueness and also

equilibrium stability analysis. Employing the then by fractional Adams-Bashforth-Moulton method, we solved numerically. the fractional model. The simulations that arose visualized the effect of disease incidence, taking into consideration values of model parameters, Caputo operator of many different fractional orders. Furthermore, we then conducted simulation of parameters like contact rate of infected people and the contact between the susceptible and the infected people. The results shown were as follows: that increased treatment strategy shall work well to reduce the Covid-19 cases among the individual population. The issues researched in Novel trial functions and rogue waves of bilinear neural network generalization of breaking soliton equations the approach proposed in [?] provided that creates a general analytic solution of Non-linear partial with analytic solution symbolic path In future one can use this method to solve differential equations work.

Funding

No funding available.

Credit authorship contribution statement

T.U. Onoja: Writing – original draft, Formal analysis. J. Amos:Supervision & Formal analysis. W. Atokolo: Writing – review, Formal analysis & editing E. Abah Software analysis. :formal review . D. Omale: Formal ariting – review & editing. G.O. Acheneje: Formal reviewing– review & editing. B. Bolaji: Formal reviewing– review & Formal analysis.

Declaration of competing interest

The authors declare that they have no known competing financial interests or personal relationships that could have appeared to influence the work reported in this paper.

References

[1] Atokolo, W., Aja, R.O., Aniaku, S.E., Onah, I.S., and Mbah, G.C.E. (2022). Approximate solution of the fractional order sterile insect technology model via the Laplace–Adomian Decomposition Method for the spread of Zika virus disease. International Journal of Mathematics and Mathematical Sciences, 2022(1), 2297630.

[2] Atokolo W., Aja R.O., Omale D., Ahman Q.O., Acheneje G.O., and Amos, J.(2024). Fractional mathematical model for the transmission dynamics and control of Lassa fever Journal of journal homepage: www.elsevier. 2773-1863/© 2024com/locate/fraopehttps:// doi.org/10.1016/j.fraope.2024.100110.

[3] Acheneje, G.O., Omale, D., Agbata, B.C., Atokolo, W., Shior, M.M., and Bolarinwa, B. (2024). Approximate solution of the fractional order mathematical model on the transmission dynamics on the co-infection of COVID-19 and Monkeypox Using the Laplace-Adomian Decomposition Method. International Journal of Mathematics and StatisticsStudies,12(3), 17-51.

[4] Atokolo W., Omale D., Tenuche, S., Olayemi S.K., Alih D., and Akpa J. (2020). Mathematical model of the transmission dynamics of Corona Virus Disease (COVID-19) and its control. Asian Research Journal of Mathematics.

[5] Amos J., Omale D., Atokolo W., Abah E., Omede B.I., Acheneje G.O., and Bolaji B. (2024), Fractional mathematical model for the Transmission Dynamics and control of Hepatitis C,FUDMA Journal of Sciences,Vol.8,No.5,pp.451-463, DOI: https://doi.org/10.33003/fjs-2024-0805-2883.

[6] James P., Omale D., Atokolo W., Amos J., Acheneje G.O., and Bolaji B. (2024), Fractional mathematical model for the Transmission Dynamics and control of HIV/AIDs,FUDMA Journal of Sciences,Vol.8,No.6,pp.451-463, DOI: https://doi.org/10.33003/fjs-2024-0805-2883.

[7] Abah E., Bolaji B., Atokolo W., Amos J., Acheneje G.O., Omede B.I, Amos J., and Omeje D. (2024), Fractional mathematical model for the transmission dynamics and control of Diphtheria. International Journal of Mathematical Analysis and Modelling, Vol.7.

[8] Ullah A.Z., Abdeljawad T., Hammouch Z., and Shah K. (2020). A hybrid method for solving fuzzy Volterra integral equations of separable type kernels, J. King Saud Univ. Sci., 33. http://dx.doi.org/10.1016/j.jksus.2020.101246.

[9] Yunus, A.O., Olayiwola, M.O., Adedokun, K.A., Adedeji, J.A., and Alaje, I.A. (2022). Mathematical analysis of fractional-order Caputo's derivative of coronavirus disease model via Laplace Adomian decomposition method. Beni-Suef University Journal of Basic and Applied Sciences, 11(1), 144.

[10] Ahmed I., Goufo E.F.D. , Yusuf A., Kumam P., Chaipanya P., and Nonlaopon K. (2021). An epidemic prediction from analysis of a combined HIV-COVID-19 co-infection model via ABCfractional operator. Alexandria Engineering Journal, 60(3), 2979–2995.

[11] Bonyah E. and Zarin R. (2020). Mathematical modeling of Cancer and Hepatitis co-dynamics with non-local and nonsingular kernal. https://doi.org/10.28919/cmbn/5029.

[12] Baskonus H.M. and Bulut H. (2015). On the numerical solutions of some fractional ordinary differential equations by fractional Adams Bashforth-Moulton Method, Open Math. 13, 1.

[13] Diethelm K. (1999). The FracPECE subroutine for the numerical solution of differential equations of fractional order.